

University of Groningen

Whole lifespan microscopic observation of budding yeast aging through a microfluidic dissection platform

Lee, Sung Sik; Avalos Vizcarra, Ima; Huberts, Daphne H E W; Lee, Luke P; Heinemann, Matthias

Published in:

Proceedings of the National Academy of Sciences of the United States of America

DOI:

[10.1073/pnas.1113505109](https://doi.org/10.1073/pnas.1113505109)

IMPORTANT NOTE: You are advised to consult the publisher's version (publisher's PDF) if you wish to cite from it. Please check the document version below.

Document Version

Publisher's PDF, also known as Version of record

Publication date:

2012

[Link to publication in University of Groningen/UMCG research database](#)

Citation for published version (APA):

Lee, S. S., Avalos Vizcarra, I., Huberts, D. H. E. W., Lee, L. P., & Heinemann, M. (2012). Whole lifespan microscopic observation of budding yeast aging through a microfluidic dissection platform. *Proceedings of the National Academy of Sciences of the United States of America*, 109(13), 4916-4920. <https://doi.org/10.1073/pnas.1113505109>

Copyright

Other than for strictly personal use, it is not permitted to download or to forward/distribute the text or part of it without the consent of the author(s) and/or copyright holder(s), unless the work is under an open content license (like Creative Commons).

The publication may also be distributed here under the terms of Article 25fa of the Dutch Copyright Act, indicated by the "Taverne" license. More information can be found on the University of Groningen website: <https://www.rug.nl/library/open-access/self-archiving-pure/taverne-amendment>.

Take-down policy

If you believe that this document breaches copyright please contact us providing details, and we will remove access to the work immediately and investigate your claim.

Downloaded from the University of Groningen/UMCG research database (Pure): <http://www.rug.nl/research/portal>. For technical reasons the number of authors shown on this cover page is limited to 10 maximum.

Supporting Information

Lee et al. 10.1073/pnas.1113505109

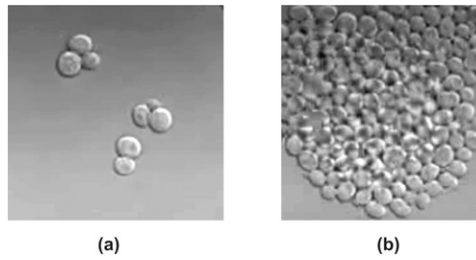


Fig. S1. Illustration of difficulty of long-term microscopic monitoring of mother yeast cells without bud removal. (A) Beginning. (B) After approximately six generations tracking of old mother cells is almost impossible.

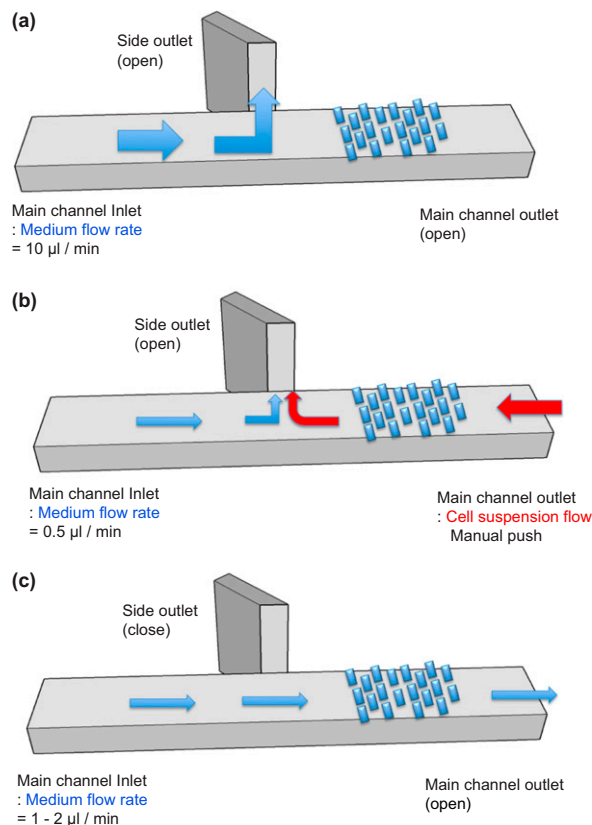


Fig. S2. Illustration of the cell loading and cultivation procedure. (A) Priming first half of main channel with medium, (B) cell loading and fixation in the cell trap array, and (C) cultivation. The microfluidic device consists of a straight main channel with an inlet and outlet, and a side channel between the two inlets. The main channel contains the cell trap array. The side channel branches off between the inlet channel and the micropad array. The fluidic resistance of the side channel (height = 100 μm) is lower than that of the main channel (height = 15 μm), which helps to control the direction of the medium and cell suspension flow during the cell-loading procedure. To prevent air bubbles and dirt from entering the microfluidic device, which is a critical issue with long-term experiment, all solutions were filtered before use. In addition, a syringe filter (pore size: 0.20 μm) was placed between the syringe for media flow and the inlet tubing and the air bubbles in the syringe were removed before it was connected to the tubing. The experimental procedure consists of three steps: inlet channel priming with media, cell loading and fixation in the cell trap array, and cultivation. Generally, inlets were closed by stopping the flow through this inlet (i.e., either by switching off the syringe pump or by removing any applied force on the syringe with cell suspension). Outlets are closed by insertion of a metal plug. (A) Inlet channel priming with media: First, the channels upstream of the cell trap array are primed with cultivation media to remove all air from the microfluidic channel. The media flow (flow rate = 10 $\mu\text{L}/\text{min}$) is applied by a syringe pump connected to the inlet. The cell trap array with its polydimethylsiloxane (PDMS) pads has a much larger resistance than the side channel. Therefore, the media flow tends to stream out the side channel, and the upstream of the array is completely filled with media flow, leaving the cell trap array and outlet channel dry. (B) Cell loading and fixation in the cell trap array: In the second step, the cell loading and fixation process is achieved by introducing cell suspension ($\text{OD}_{600} = 0.3$) through the outlet of the main channel (by manually pushing a syringe containing the cell suspension), while the media flow through the inlet is maintained, but the flow rate is reduced to 0.5 $\mu\text{L}/\text{min}$. As a result, both flow directions are toward the side channel, and the cells that are not trapped underneath the pads do not settle down at the upstream of the array but wash out through the side channel. This procedure prevents contamination and growth of cells upstream of the cell culture array during long-term experiments, which could lead to blocking of the inlet and the main channel with cells. In this procedure, air is also efficiently pushed out of the cell trap area into the side channel through which it exits the chip. Residual air that accumulates at the interface of the opposing flow of media and cell suspension serves as a pressure buffer during the subsequent closure of the side channel. This procedure ensures that the trapped cells keep their positions during the change of pressure induced by flow changes. (C) Cultivation: As a final step, as soon as the cell loading density in the cell trap array is sufficient (e.g., fewer than three mother cells per pad), the flow of the cell suspension is stopped and the side channel is closed by insertion of a metal plug. At the same time, the flow through the inlet channel is set to the final flow rate (1–3 $\mu\text{L}/\text{min}$). The closure of the side channel results in increased pressure in the main channel, leading to removal of residual air bubbles between the inlet and side channel through the gas-permeable PDMS layer. Following this procedure, the whole chip is scanned to make sure that no bubbles remain in the device.

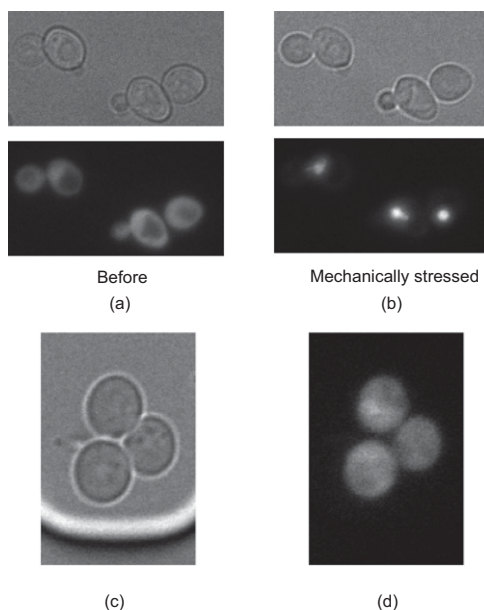


Fig. S3. (A) Cells between a glass slide and layer of PDMS (with a 40- μ m distance); here Msn2 is localized in the cytoplasm. (B) The same cells after applying severe external pressure on the PDMS layer; here Msn2 localizes to the nucleus indicating that Msn2 localization can indeed indicate physical stress. (C) Bright-field and (D) fluorescent images of cells under a PDMS elastic pad of our microfluidic chip, where Msn2 is localized in the cytoplasm. A potential issue with our setup could have been stress imposed on the cells by the mechanical force applied by the micropad. Generally, we did not expect the cells to be stressed because a similar type of micropad has already been used for budding yeast cells without this complication (1–3); however, we aimed to show experimentally that the setup indeed does not stress the cells. For this purpose, we used a yeast strain that had a GFP fused to the general stress-responsive transcriptional activator Msn2. Msn2 localizes to the nucleus under stress conditions (4). We found that the Msn2-GFP protein is localized in the cytoplasm of cells underneath the micropad. In a control experiment in which we manually squeezed the PDMS pad and thus the cell, the fusion protein localized to the nucleus, indicating that during regular operation of the chip, the cells are not stressed.

1. Cookson S, Ostroff N, Pang WL, Volfson D, Hasty J (2005) Monitoring dynamics of single-cell gene expression over multiple cell cycles. *Mol Syst Biol* 1:2005.0024.
2. Lee PJ, Helman NC, Lim WA, Hung PJ (2008) A microfluidic system for dynamic yeast cell imaging. *Biotechniques* 44:91–95.
3. Dechant R, et al. (2010) Cytosolic pH is a second messenger for glucose and regulates the PKA pathway through V-ATPase. *EMBO J* 29:2515–2526.
4. Schmitt AP, McEntee K (1996) Msn2p, a zinc finger DNA-binding protein, is the transcriptional activator of the multistress response in *Saccharomyces cerevisiae*. *Proc Natl Acad Sci USA* 93:5777–5782.

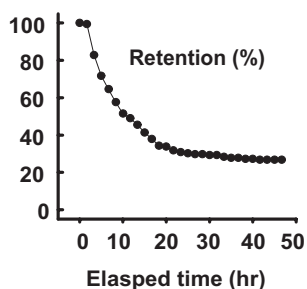
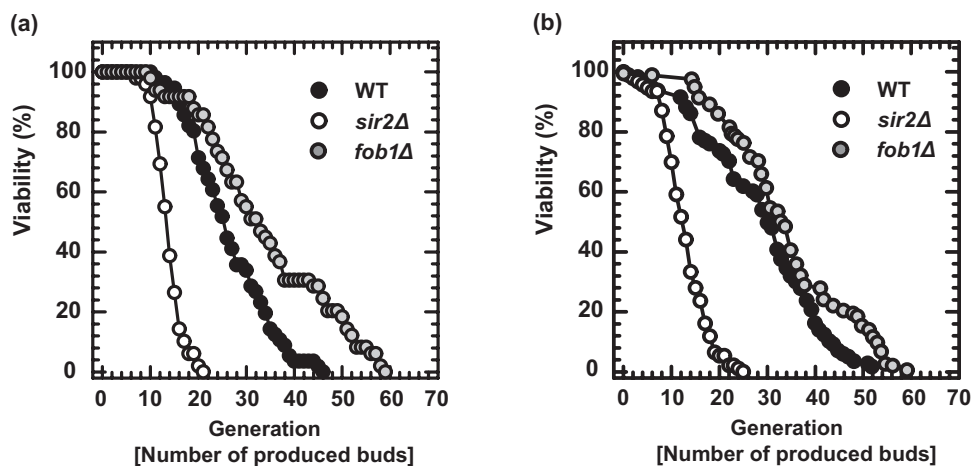


Fig. S4. Retention of cells under micropad. The plot shows the percentage of retained cells as a function of the elapsed experimental time.



	Microfluidic dissection		Conventional dissection	
	Median lifespan	Maximum lifespan	Median lifespan	Maximum lifespan
WT	25	45	30	52
<i>sir2Δ</i>	13	21	13	25
<i>fob1Δ</i>	32	58	34	59

Fig. S5. Side-by-side comparison of replicative lifespans obtained with (A) microfluidic dissection and (B) conventional dissection. For both types of experiments, the strains were grown overnight in YPD medium to stationary phase and then allowed to resume exponential growth by dilution into fresh YPD medium, and incubation for 3 h at 30 °C before the experiment. The numbers of analyzed cells for the microfluidic dissection platform were WT: $n = 56$; *sir2Δ*, $n = 48$; *fob1Δ*, $n = 49$, respectively. The data obtained with the classic dissection method was taken from Shcheprova et al. (1) (WT and *fob1Δ*) or was kindly provided by the group of Yves Barral (*sir2Δ*).

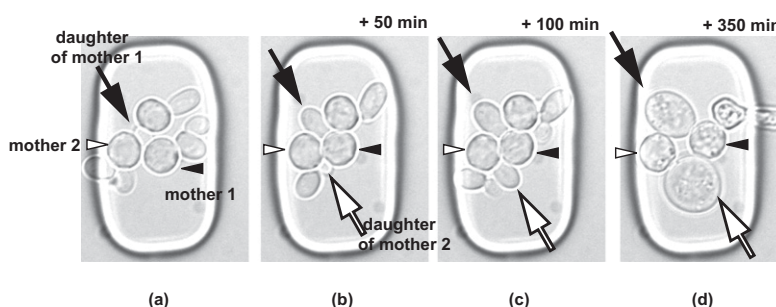
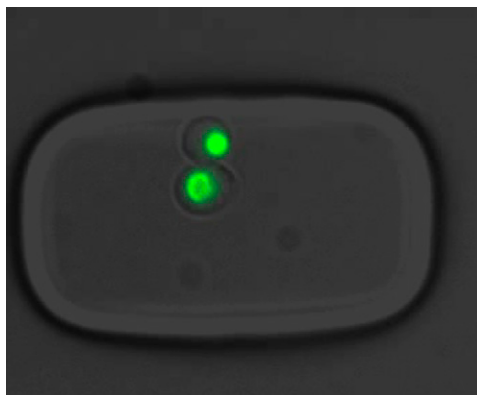
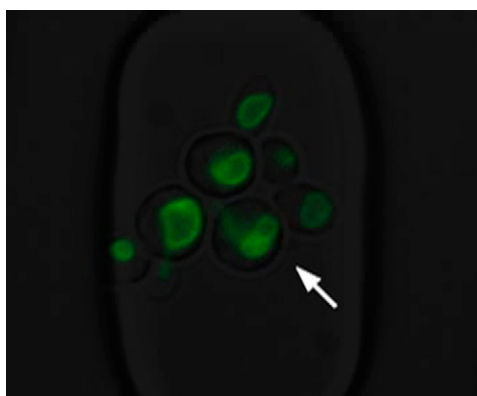


Fig. S6. Image of huge daughter cells compared to their mothers. Arrowheads and arrows point out mother and daughter cells, respectively. (A) Mother cell 1 (filled arrowhead) had produced 20 buds; mother cell 2 (unfilled arrow head) had produced 22 buds. (B–D) Lapsed time: 50, 100, and 350 min, respectively.



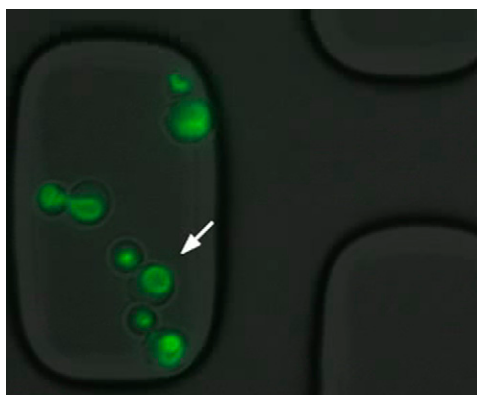
Movie S1. Example of microfluidic dissection. This movie shows a lifespan of a yeast cell, which produced 28 buds and died. Through the prealigned single focal plane of the microfluidic dissection platform, age-associated morphological phenotypes can be observed: cell and vacuole sizes (visualized by Vph1p-GFP) gradually become larger and ellipsoidal daughter cells are produced.

[Movie S1](#)



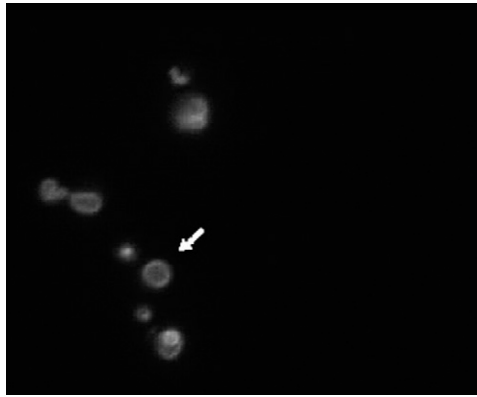
Movie S2. Example of large daughter cell. Sometimes daughter cells of old mothers were found to be bigger than mother cells. Arrows point out old mother cells: The one with the white arrow had produced 20 buds, and the one with the yellow arrow had produced 22 buds. Cells expressing Vph1p-GFP served for visualizing vacuoles.

[Movie S2](#)



Movie S3. Example of ellipsoidal (pseudohyphae)-type death pattern. The cell pointed out by the arrow shows an example of ellipsoidal death pattern. It had produced 23 buds. Cells expressing Vph1p-GFP served for visualizing vacuoles.

[Movie S3](#)



Movie S4. Same movie as [Movie S3](#), showing only the fluorescence channel. The vacuole pointed out by arrows belongs to the same as indicated in [Movie S3](#). The vacuole size gradually becomes larger; at some point it fails to complete the fusion processes after cell division and a fragmented vacuolar structure can be observed. Cells expressing Vph1p-GFP served for visualizing vacuoles.

[Movie S4](#)



Movie S5. Example of spherical-type death pattern. In the movie, the cell produced 14 buds and died without significant cell morphology change. A ruptured-like vacuole was observed at the end of the cell's life. Cells expressing Vph1p-GFP served for visualizing vacuoles.

[Movie S5](#)